

Photonics applications I



- ✓ Attributes of ChG for photonics applications
- ✓ Transmission window
- ✓ IR transmitting lens

Useful attributes for photonics

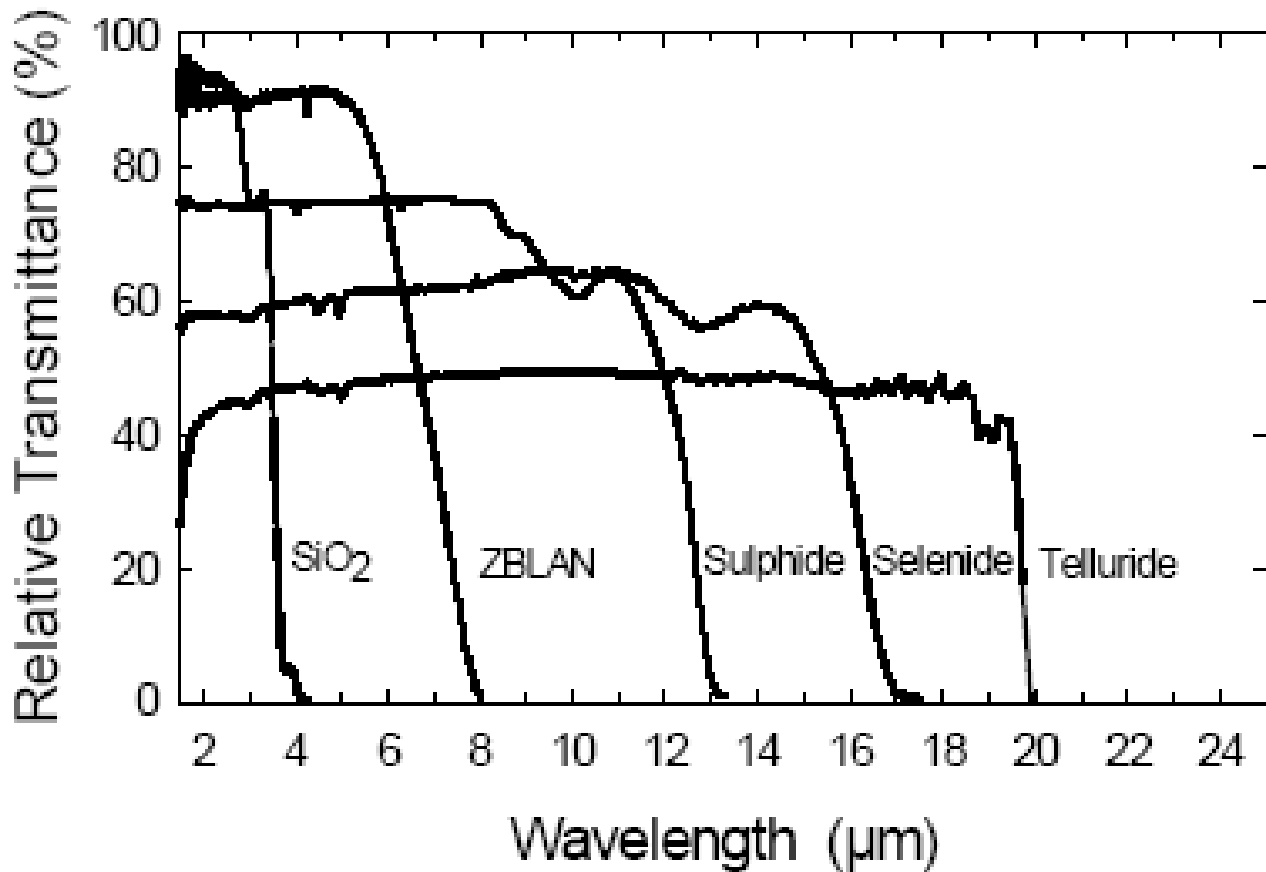
- High refractive index over wavelengths useful in photonics and optical communications
- Low phonon energy for reducing multiphonon relaxation of excited state of doped ions
- Wide optical transmission window extended to mid IR
- Strong photosensitivity: photoinduced changes in n and α , photoinduced (vectorial) dichroism, photoinduced volume expansion and fluidity, photodissolution of Ag, photoinduced differential etching, and so on
- High third order optical susceptibility for nonlinear optical applications
- Large acousto-optic effect
- Low processing temperatures compared to other conventional glasses









Photonics applications: classification

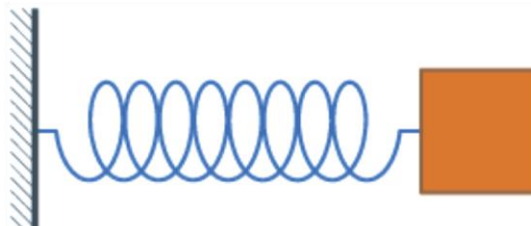
- ✓ **Passive applications; IR transmission, waveguide**
 - IR transmitting window, lenses, fibers...
 - Photoinduced optical waveguides, Ag-photodissolved waveguides, photoetched waveguides...
 - Bragg diffraction gratings, polarization gratings, holographic recordings, photonic crystals (3D Bragg gratings)...

- ✓ **Active applications; undoped or doped**
 - Optical amplifiers and lasers; RE-activated, SRS, SBS...
 - Optical devices; all-optical ultrafast nonresonant-type optical switches
 - Photoresists for photolithography

Infrared transmission



VIA 16	VIIA 17
 16,0 8 O	 19,0 9 F
 32,1 16 S	 35,5 17 Cl
 79,0 34 Se	 79,9 35 Br
 127,6 52 Te	 126,9 53 I



$$F_s = -kx$$

$$f_n = \frac{1}{2\pi} \sqrt{\frac{k}{m}}$$

IR-side absorption

- ✓ Due to the combination of vibrations and higher harmonics (multiphonon absorption) of the short-range order units.
- ✓ Essentially continuous phonon spectrum toward longer wavelengths due to the structural disorder.
- ✓ ChGs consist of relatively heavy elements and the chemical bonds are usually weaker than oxide glasses.

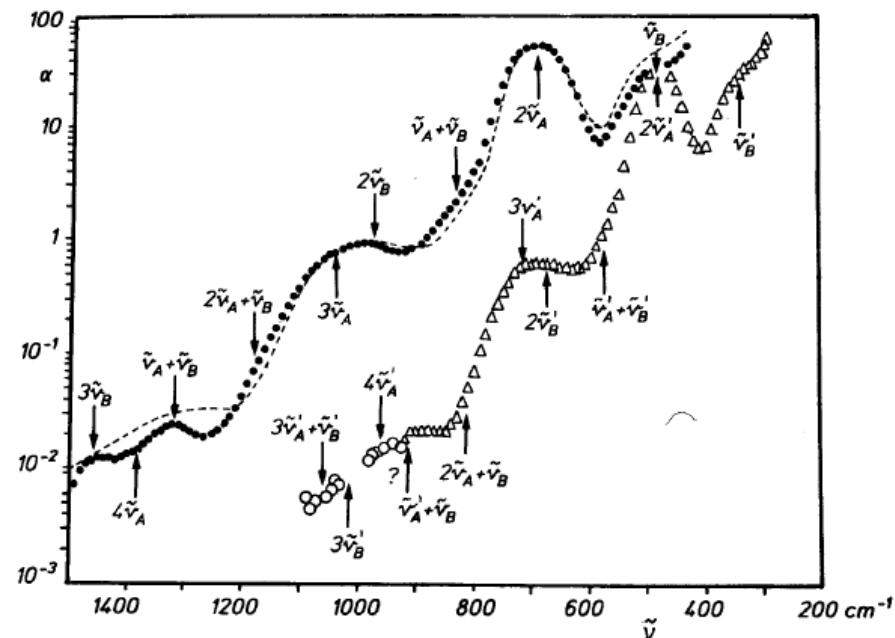


Fig. 4.38. Absorption coefficient α in the region of the fundamental and higher harmonics or combination vibrations for vitreous As_2S_3 and As_2Se_3 .

Transmission window

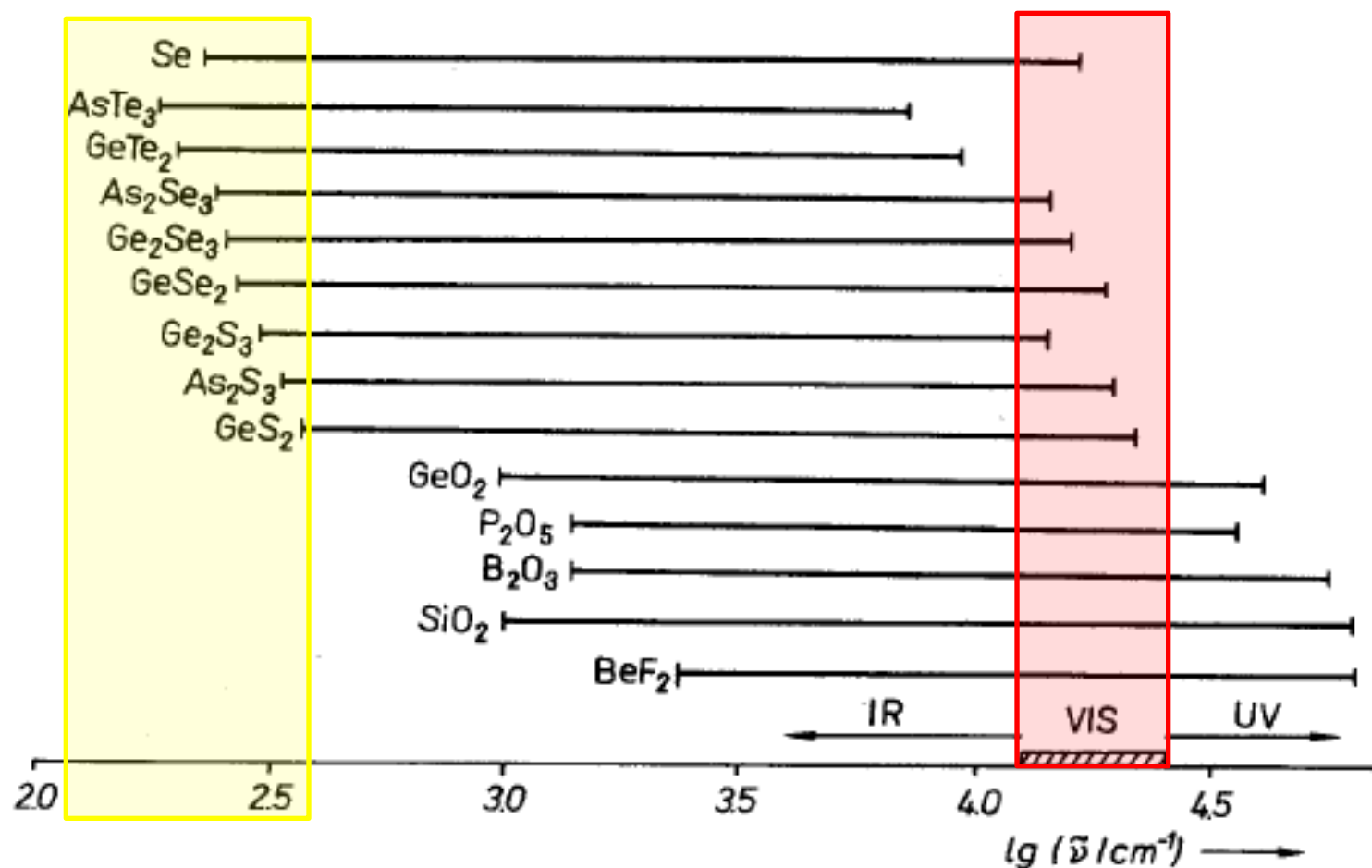


Fig. 4.37. Wavenumber interval between the fundamental vibration band with the highest frequency and the absorption edge ($\alpha = 10^4 \text{ cm}^{-1}$) for characterizing glass-forming compounds as optical media.

Effects of impurities

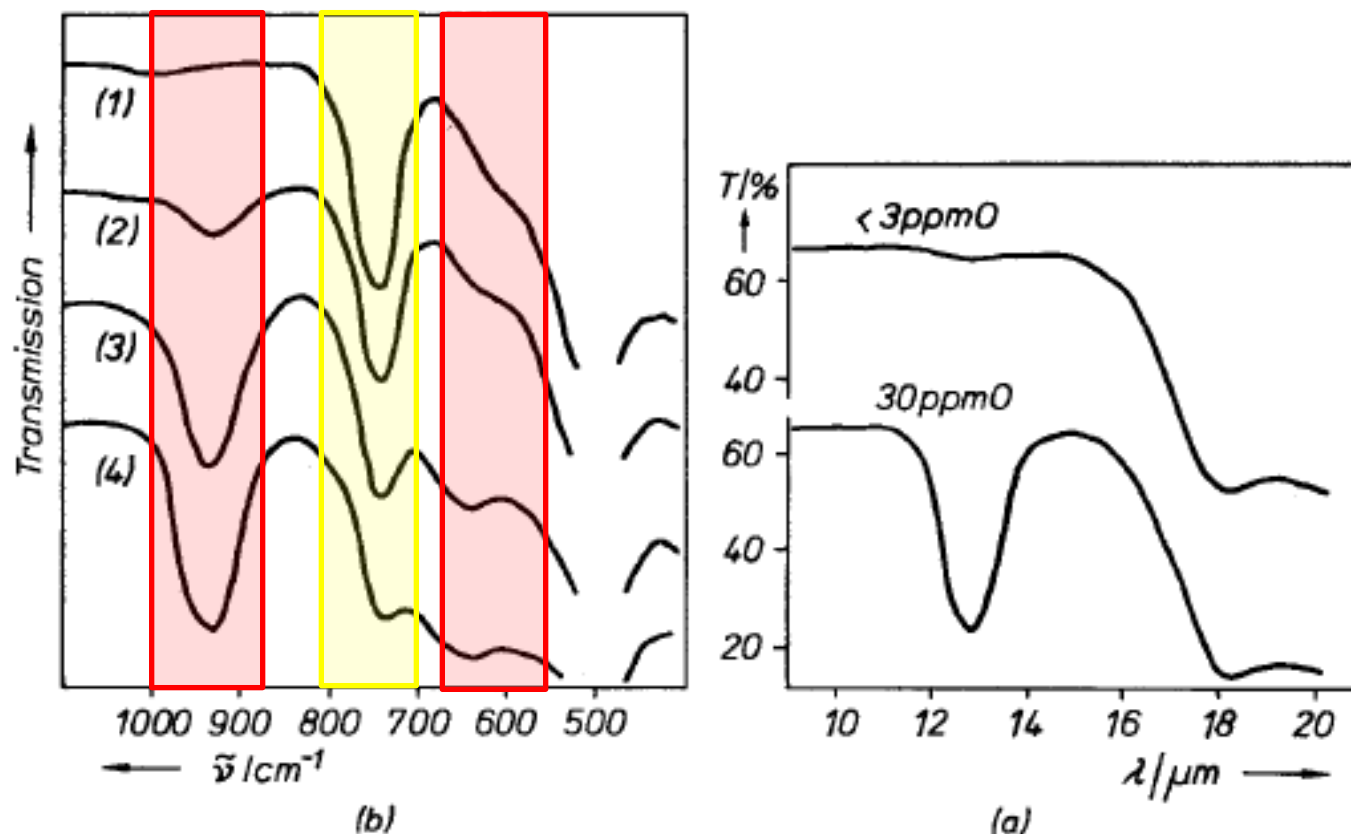
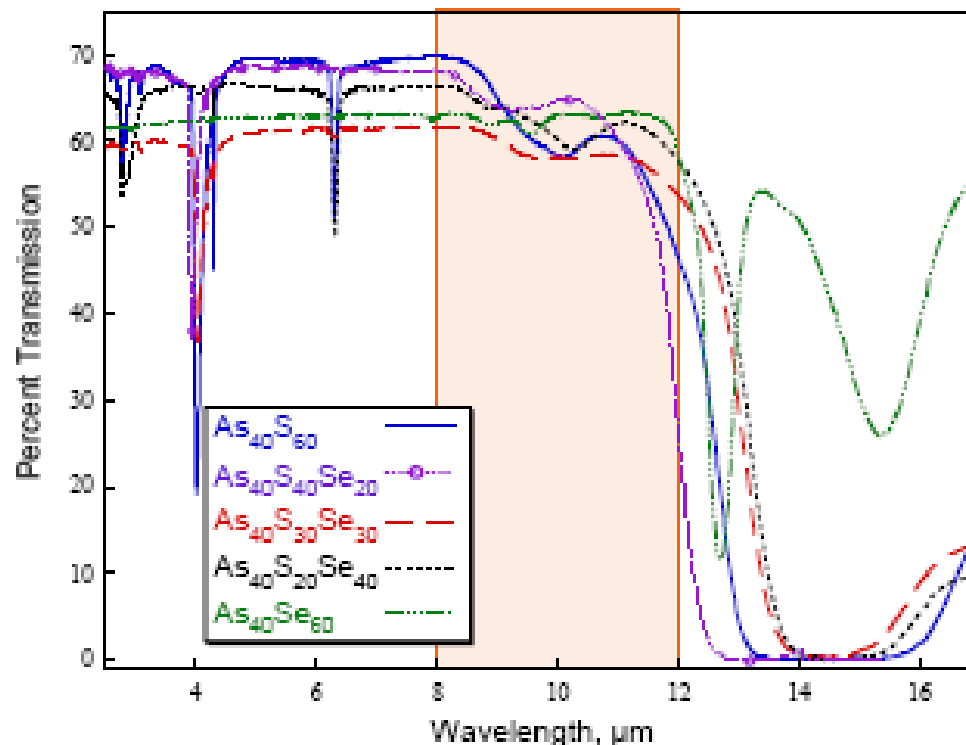


Fig. 4.40. Effects of small quantities of oxide on the transmission spectrum of vitreous selenium.

(a) Transmission spectrum in the region of the absorption band caused by oxide impurities.

(b) Absorption spectra of vitreous selenium samples

with different oxide contents [4.258]. (1) pure Se ($d = 15.5\text{ mm}$), (2) Se with $7.4 \times 10^{-4} \% \text{ O}$ ($d = 15.5\text{ mm}$), (3) Se with $11.3 \times 10^{-4} \% \text{ O}$ ($d = 13.5\text{ mm}$), (4) Se with $70.3 \times 10^{-4} \% \text{ O}$ ($d = 13.6\text{ mm}$).



Sundaram et al, Lezal et al, Pacific Northwest National Lab.

Compound	Bond	Position [nm] and intensity
As ₂ O ₃	As-O	7.90 s, 9.50 w, 12.34 vs
GeO ₂	Ge-O	10.40 m, 10.77 s, 11.40 vs
SiO ₂	Si-O	9.27 vs, 12.50 m
SeO ₂	Se-O	10.06 vs, 13.96 s
H ₂ S	H-S	4.01 s, 3.70 m, 2.54 w
H ₂ Se	H-Se	4.57 s, 4.12 m, 3.53 w
OH group	O-H	2.93 vs, 2.78 m, 2.24 m
Carbonate	C-H	3.50 m, 3.41 m
H ₂ O	O-H	6.30 s

Intensity of absorption bands: vs – very strong, s – strong, m – middle, w – weak, vw - very weak

Some IT transmitting materials

Material	Transmission range μm	IR abs. coeff. cm^{-1} (at 10.6 μm or as stated)	Hardn. (Knoop)	$\frac{n}{(5 \mu\text{m})}$	$\frac{dn}{dT}$ 10^6 K
KBr	0.23–26	1.2×10^{-4} (3 μm)	7	1.533	-40
NaCl	0.2 –15	7×10^{-6} (1.06 μm)	15	1.519	-33
KRS-5	0.6 –40	—	40	2.38	-236
Si	1.2 – 8	0.01 (2.5 μm)	1100	3.4261	40
Ge	1.8 –23	1.3×10^{-3} (2.7 μm)	800	4.015	500
Al_2O_3	0.7 –4.5	4×10^{-4} (2.5 μm)	1370	1.6677	13
GaAs	1 –16	<0.01	721	3.2975	147
ZnS	1 –12	0.15	178	2.28 (1.4 μm)	42
ZnSe	0.5 –22	0.03	137	2.405 (10 μm)	48
CdTe	0.9 –15	1×10^{-3}	56	2.684	50
$(\text{La}_2\text{S}_3)_{90}(\text{CaS})_{10}$	0.7 –15	0.1	570	—	—
vit. As_2S_3	0.6 –11	—	109	241	-10
vit. As_2Se_3	1.0 –15	1.5×10^{-2}	114	2.79	—
$\text{Ge}_{33}\text{As}_{12}\text{Se}_{55}$	0.7 –14	5×10^{-2}	170	2.51	-85
$\text{Ge}_{28}\text{Sb}_{12}\text{Se}_{60}$	0.7 –14	10^{-2}	150	2.62	+80

Some IR transmitting ChGs

Table 5.5. Optical properties of infrared-transmitting glasses of the AMTIR series produced by Amorphous Materials, Inc.

Glass type	n 25°C	$10^6 dn/dT/K^{-1}$ 25-(−197) (25–150)	α cm^{-1}	β $g \cdot cm^{-3}$	$10^6 \alpha$ K^{-1}	Hardn. (Knoop)	Tensile modulus psi	$\lambda s \cdot cm \cdot K$ cal	ρ Ωcm	T_G K
AMTIR 3	2.6266	58	0.002	4.67	13.5	150	3.2×10^6	5.3×10^{-4}	5×10^{11}	551
Ge-Sb-Se	(3 μm)	(98)								
	2.6173	57	0.001							
	(5 μm)	(92)								
	2.6117	56	0.001							
	(7 μm)	(90)								
	2.6055	56	0.004							
	(9 μm)	(89)								
	2.5983	56	0.03							
(11 μm)	(92)									
2.5892	—	0.20								
(13 μm)	(—)									
AMTIR 1 Ge-As-Se				4.4	12	170	3.1×10^6	6×10^{-4}	2×10^{12}	635

Feltz book, p. 429.

Glass	Phonon energy (cm^{-1})	Transmission range (μm)	Refraction index
As ₂ S ₃	350	0.5-6	2.35
As ₂ Se ₃	360	0.8-12	2.7
As ₂ Te ₃	380	1.5-15	3.5
Ge ₂₀ Se ₈₀	360	0.9-12	2.35
Ge ₂₅ Ga ₁₀ S ₆₅	380	0.6-7	2.58
Ge ₂₅ Ga ₅ As ₅ S ₆₅	330	0.6-7	2.58

Lezal et al, Chalcogenide Letters, 1 (2004) 11.

UV-side absorption

- ✓ Electronic transitions between the valence and conduction bands; absorption edge, optical band gap
- ✓ The Tauc edge (@ $\alpha > 10^4 \text{ cm}^{-1}$)
 - Transitions from delocalized states in the valence band to delocalized states of the conduction band.
 - On the assumption that the energy dependence of the DOS is parabolic,

$$\alpha(\omega) = A[\hbar\omega - (E_c - E_v)^2]/\hbar\omega$$

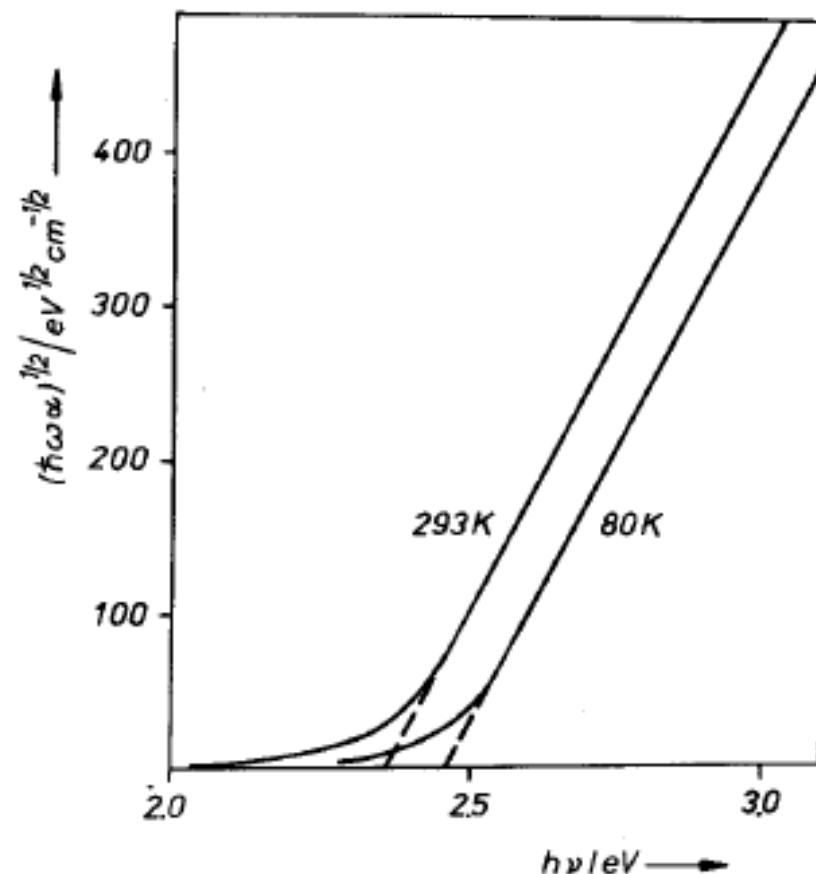


Fig. 4.44. Plot of the absorption edge for vitreous As_2S_3 at 293 K and 80 K (according to [4.280]).

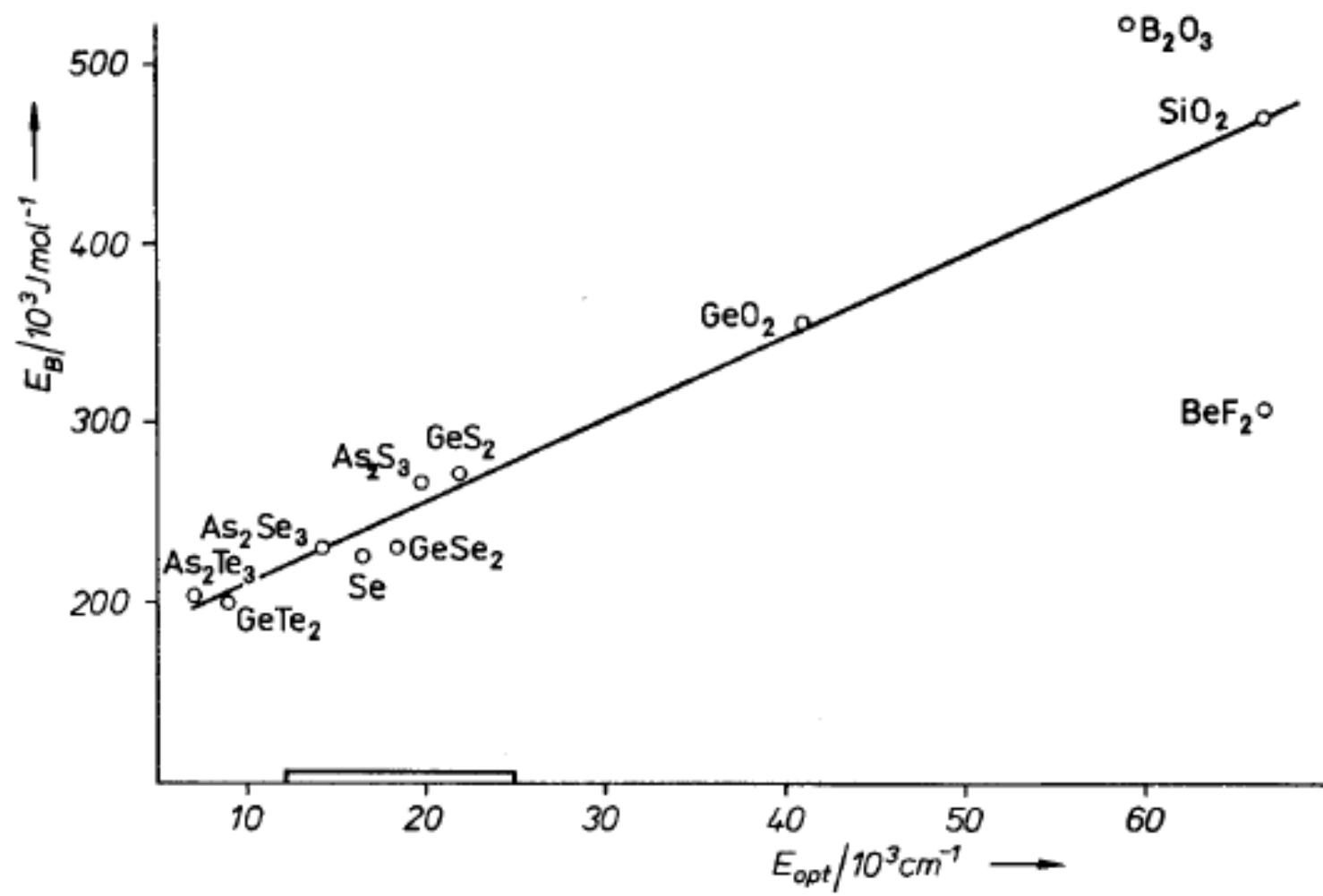


Fig. 4.45. Correlation of the average molar bonding energy with the optical band gap ($\alpha = 10^4 \text{ cm}^{-1}$) of glass-forming compounds.

UV-side absorption

✓ The Urbach edge

- The exponential section of the absorption edge;

$$\alpha = B \exp [\gamma'(\hbar\omega - E_{\text{opt}})/kT]$$

- ✓ Probably caused by a freezing of potential fluctuations in the glass transition region and/or thermal fluctuations of the energy of the optical band gap.

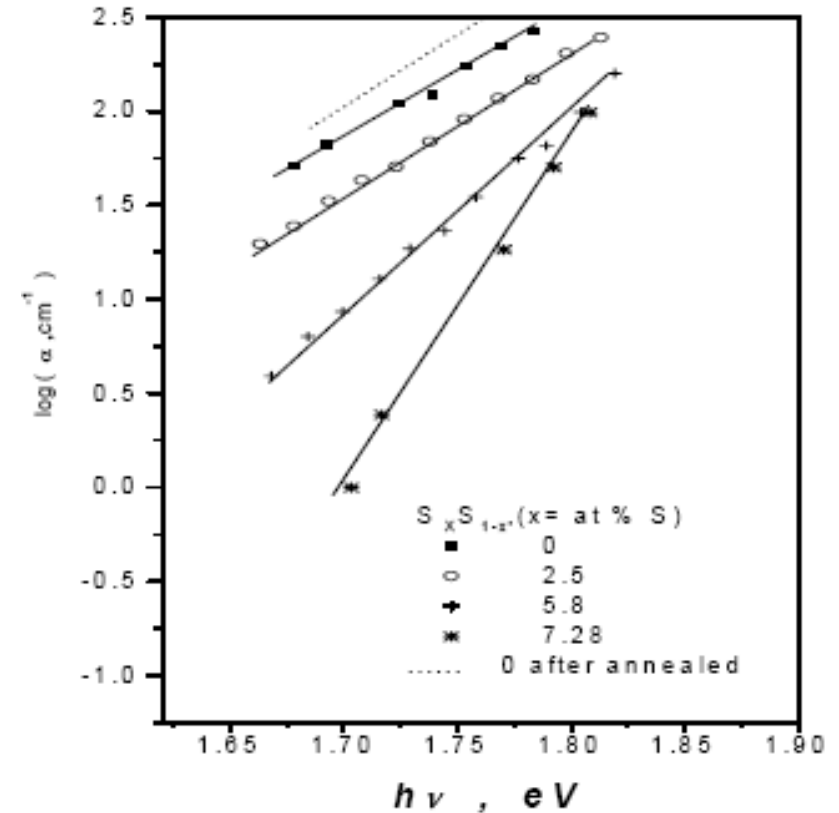


Fig. 5. Plot of $\text{Log}(\alpha)$ Versus $(h\nu)$.

Nahass et al, J. Optoelectron. Adv. Mater. 8 (2006) 1817.

UV-side absorption

- ✓ **The Weak absorption tail**
 - Another exponential dependence for the low absorption region ($\alpha < 1 \text{ cm}^{-1}$);

$$\alpha = C \exp(\hbar\omega/E_t)$$

- ✓ Probably due to the additional band gap states, which are formed from electronic impurities such as transition metal elements or defects such as valence alternation pairs and dangling bonds.*

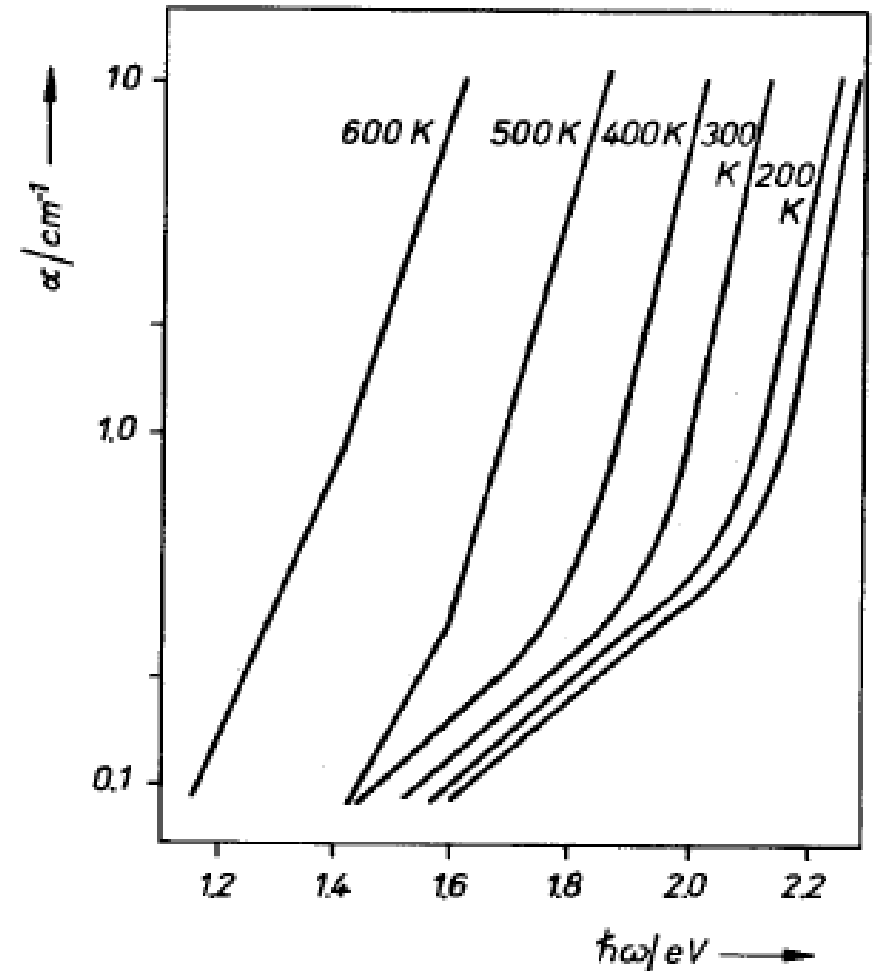


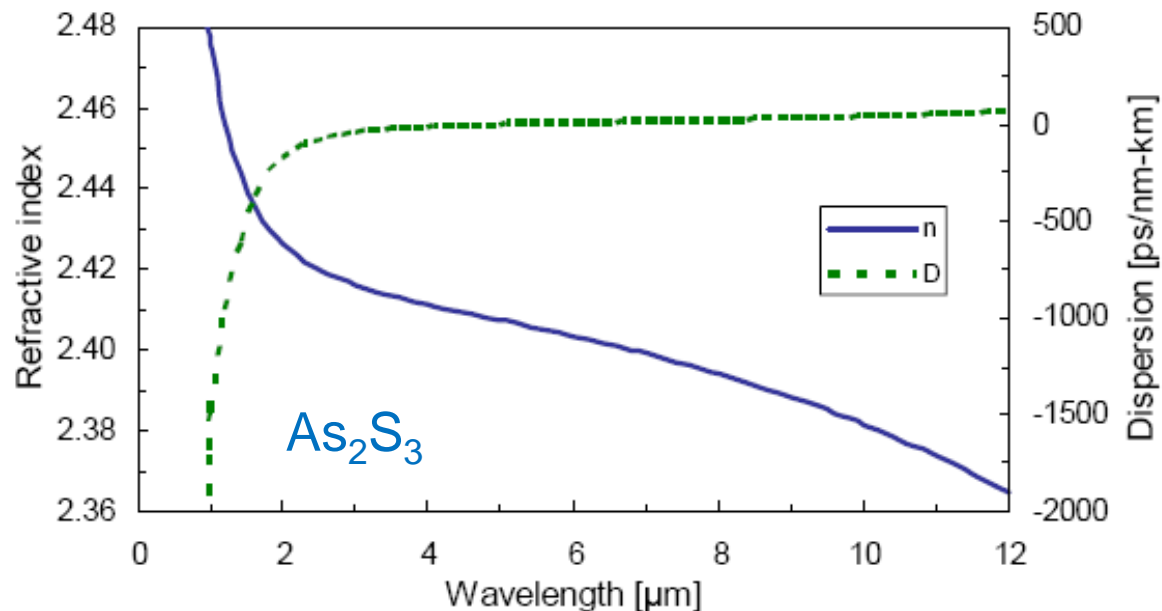
Fig. 4.48. Temperature dependence of the shape of the absorption edge in the region of small absorption coefficients for vitreous As_2S_3 (according to [4.281]).

Feltz book, p. 383.

* Wood and Tauc, Phys. Rev. B, 5 (1972) 3144.

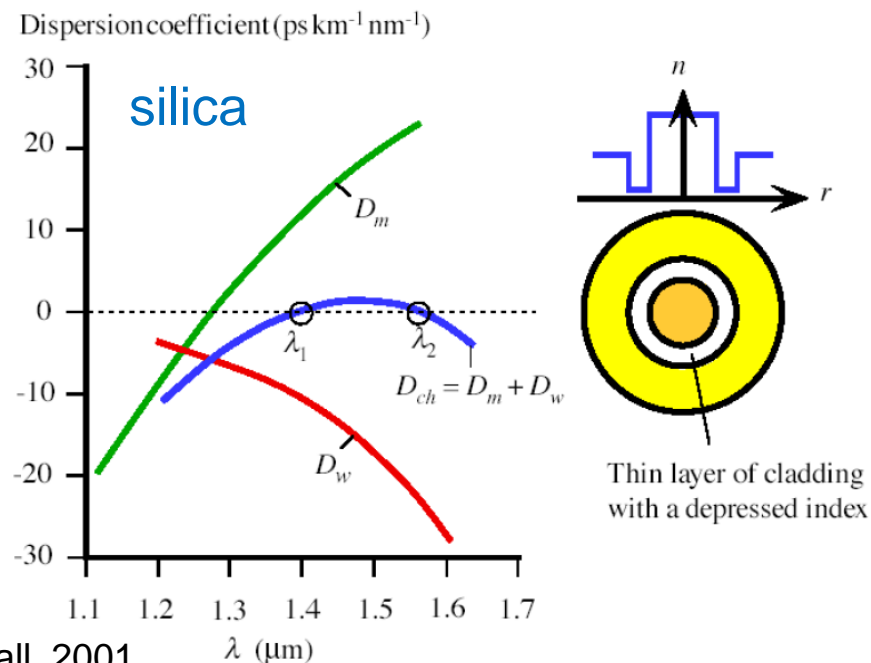
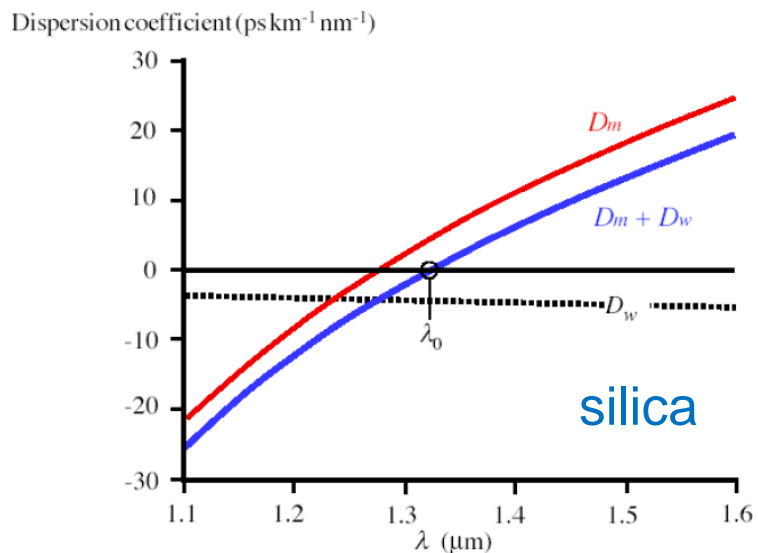
Refractive index and dispersion

- Large refractive indices between 2 to greater than 3.
- In As_2S_3 glass, n increases as sulfur is replaced by the more polarisable selenium and tellurium.
- The high n is advantageous for strong optical field confinement which allows small waveguide bend radii (leading to compact circuit designs) and enhanced optical intensities (for efficient nonlinear interactions).
- In addition, the large index contrast relative to air can potentially provide a complete band-gap for photonic crystals.



Refractive index and dispersion

- The zero dispersion wavelength for chalcogenide glasses (material dispersion) lies well in the mid IR (e.g. 5 μm for As_2S_3).
- At communication wavelengths around 1.55 μm these materials exhibit strong normal dispersion (i.e. not anomalous).
- This is not necessarily detrimental to performance as typical device lengths are short, of the order of centimeters.
- Furthermore, there is the possibility of using waveguide dispersion to engineer the chromatic dispersion, similar to what has been achieved in silica.



Measured refractive indexes were analyzed by using the Wemple equation based on the single electronic oscillator model in the region from UV to near-infrared as [9]

$$n^2 - 1 = \frac{E_d E_0}{E_0^2 - E^2}, \quad (1)$$

where n is the refractive index, E the photon energy, E_0 the average electronic energy gap and E_d the electronic oscillator strength. Larger refractive index is derived from small E_0 and/or large E_d , according to Eq. (1). Since there are some elec-

Measured refractive indexes of gallium lanthanum sulfide and oxy sulfide glasses in the region of 0.48–1.71 μm

Wavelength (μm)	Refractive index (± 0.002)	
	70Ga ₂ S ₃ ·30La ₂ S ₃	70Ga ₂ S ₃ ·30La ₂ O ₃
0.48000		2.376
0.49160		2.367
0.49219		2.366
0.50157		2.360
0.50858		2.353
0.54610	2.522	2.330
0.57897	2.500	2.315
0.58756	2.493	2.311
0.64385	2.467	2.292
0.65627	2.462	2.289
0.66784	2.458	2.286
0.70652	2.446	2.277
1.01398	2.398	2.241
1.36731	2.379	2.226
1.71010	2.371	2.219

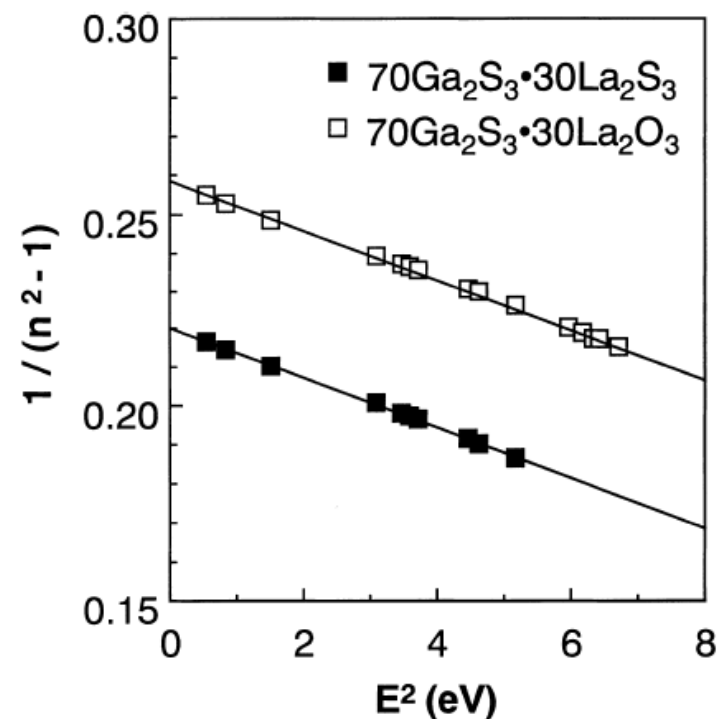


Fig. 1. Relationship between $1/(n^2 - 1)$ and E^2 for Wemple analysis. Linear functions, $1/(n_i^2 - 1) = A_i + B_i E^2$ with $i \equiv \square$ and \blacksquare , fitted to the data are represented by the lines.

Refractive indexes and material parameters of chalcogenide, oxysulfide, oxide and fluoride glasses

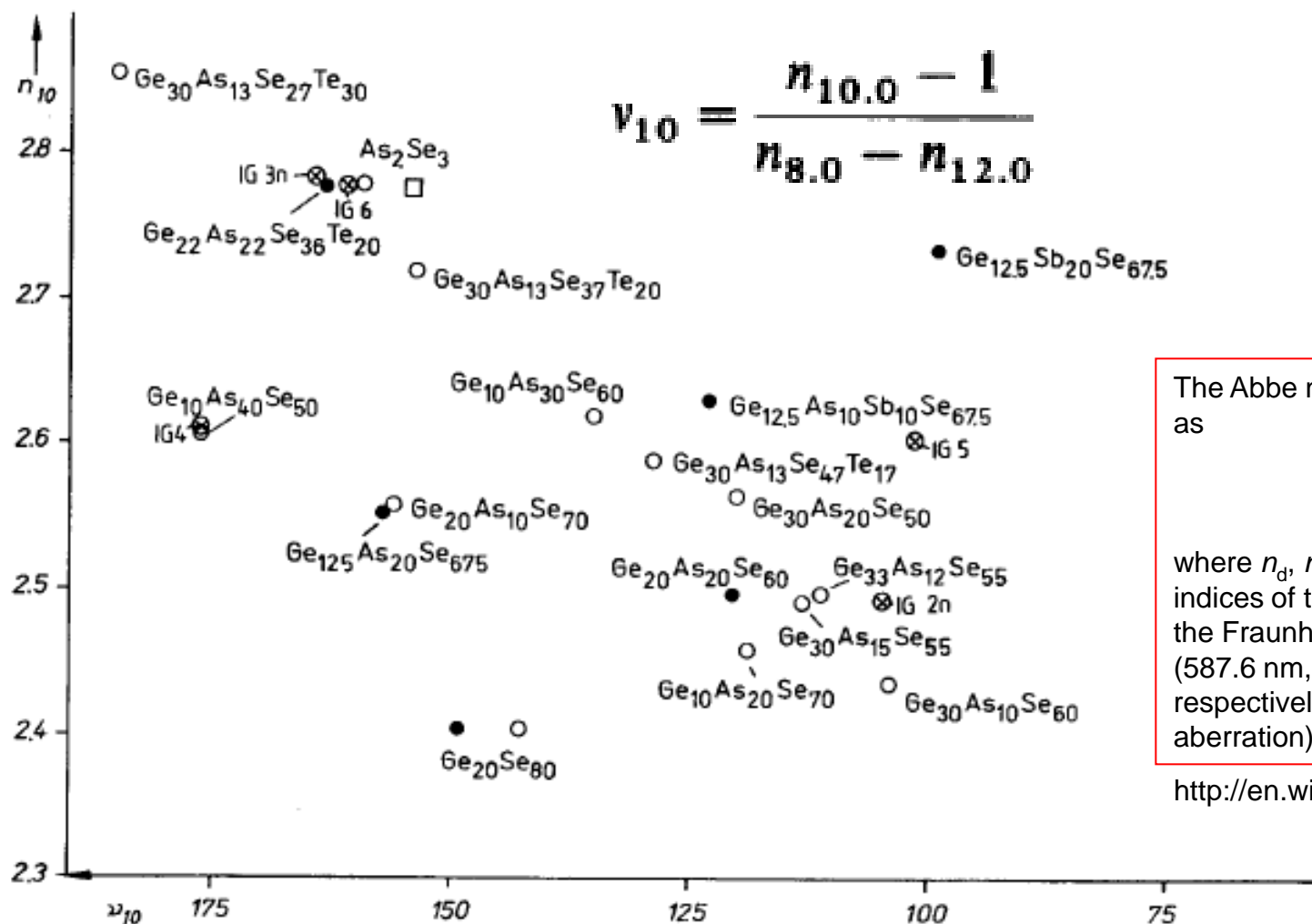
Material	Refractive index	E_0 (eV)	E_d (eV)
70Ga ₂ S ₃ ·30La ₂ S ₃	2.493 ^a	5.9 ± 0.5	26.7 ± 0.5
70Ga ₂ S ₃ ·30La ₂ O ₃	2.311 ^a	6.4 ± 0.5	24.6 ± 0.5
Ge ₃₀ S ₇₀	2.156 ^a	5.8	18.2
As ₄₀ S ₆₀	2.650 ^a	4.7	22.8
Ge ₂₅ Se ₇₅	2.37 ^b	4.5	20.9
Ge ₂₈ Sb ₁₂ Se ₆₀	2.628 ^b	4.1	24.2
SiO ₂ (Corning 7940)	1.45849 ^a	12.4	13.6
20BaO·80TeO ₂	2.10053 ^a	6.7	20.5
40PbO·40Bi ₂ O ₃ ·20Ga ₂ O ₃	2.34640 ^a	5.4	21.7
40Tl ₂ O·40Bi ₂ O ₃ ·20Ga ₂ O ₃	2.49214 ^a	4.9	20.8
ZBLAN	1.480 ^c	13.0	15.1

^a He-d line: 0.5876 μm

^b 3 μm

^c Na-D line: 0.589 μm

Refractive index and dispersion



The Abbe number V of a material is defined as

$$V = \frac{n_d - 1}{n_F - n_C},$$

where n_d , n_F and n_C are the refractive indices of the material at the wavelengths of the Fraunhofer d-, F- and C- spectral lines (587.6 nm, 486.1 nm and 656.3 nm respectively). Low dispersion (low chromatic aberration) materials have high values of V .

http://en.wikipedia.org/wiki/Abbe_number

Fig. 4.53. n/v diagram for optical media in the 10 μm region corresponding to Equation (4.106); compositions in mole percent.

IR-transmitting lens

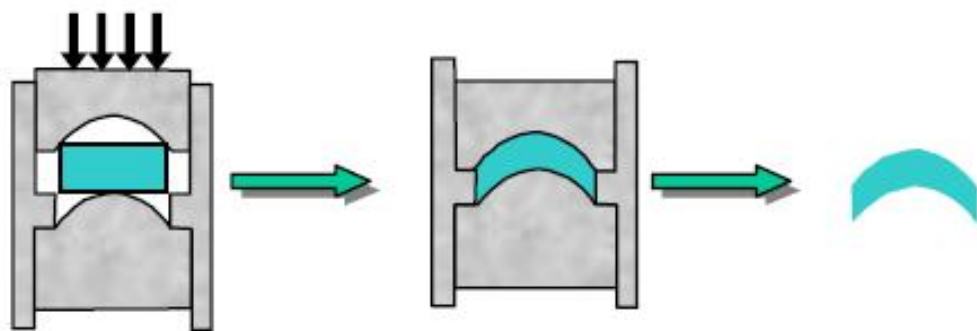


Fig. 2. Schematic representation for producing chalcogenide glass optic by molding.

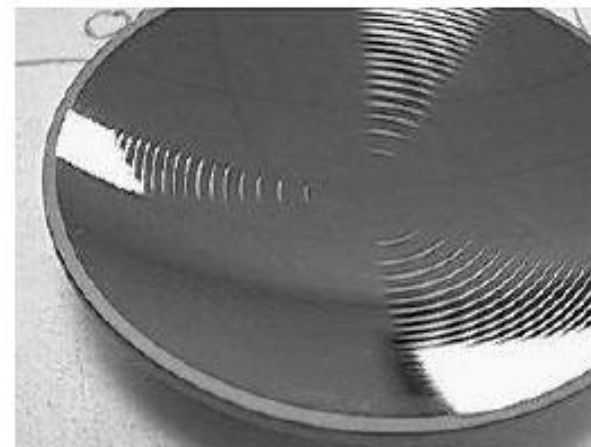


Fig. 3. Mold asphero-diffractive lens.

IR-transmitting lens

Umicore molds IR optics for night vision

Specialty materials company **Umicore**, through its business unit Electro-Optic Materials, has developed an industrial molding process, called GASIR, to manufacture low-cost infrared (IR) optics with well-controlled properties. GASIR makes commercial high-volume thermal imaging, such as automotive night vision, a

reality, according to Dimitri Van Uytfange, Application Manager Finished Optics, Umicore Electro-Optic Materials.

For many years, germanium has been the key material for thermal-imaging applications in the 8- to 12- μm wavelength, serving a wide variety of defense and commercial applications. However, the

costs associated with the germanium lenses were prohibiting their widespread usage.

“With the recent developments for cheaper infrared detector technology, Umicore realized that expensive germanium optics were one of the only factors that prevented a breakthrough for far



Umicore Electro-Optic Materials has developed an industrial molding process, called GASIR, to manufacture low-cost infrared optics for automotive night-vision systems. Replacing germanium, GASIR chalcogenide glass is a cheaper base material for the lenses.



NIR vs FIR: Positive

NIR

- + Lower sensor cost
- + Enhance all objects
- + Synergy potential with other systems such as Lane Departure function
- + Resolution higher
- + Favorable mounting location possible

FIR

- + Superior range
- + Emphasize objects at particular risk - pedestrians and animals
- + Image with lower visual clutter

NIR vs FIR: Negative

NIR

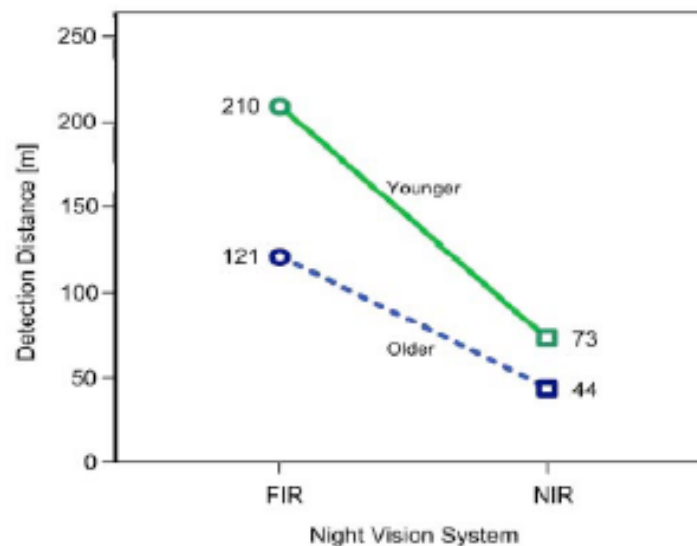
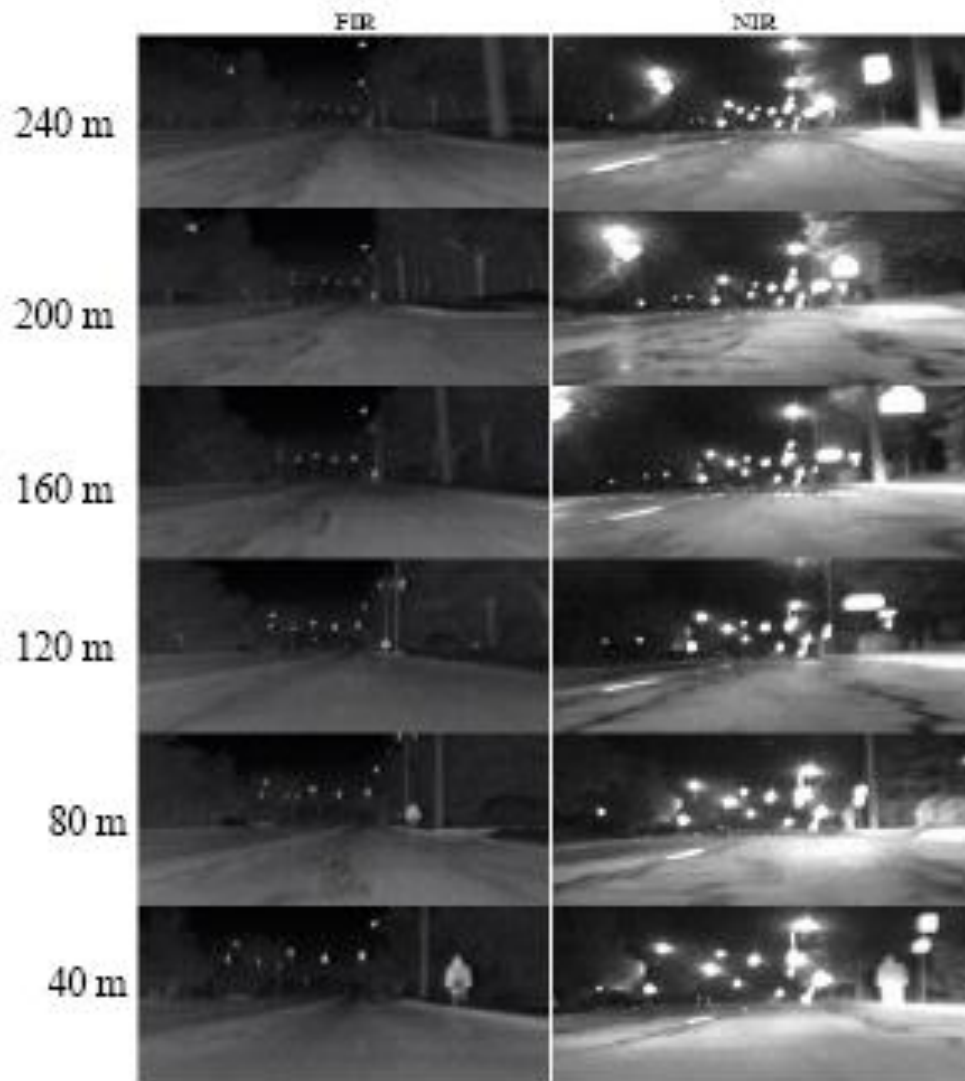
- Sensitive to glare from oncoming headlights and other NIR systems
- Detection range depend on reflectivity of object (clothing)

FIR

- Less favorable mounting location
- Image perceived as unusual
- Lower contrast for objects of ambient temperature

Easier detection using FIR

Pedestrian detection



Low-cost FIR bolometer camera

Today



High end BMW night vision based on conventional FIR technology

PIMS

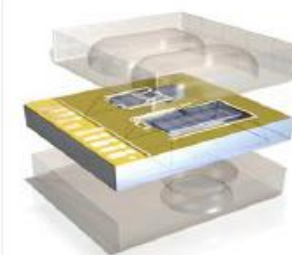


Future

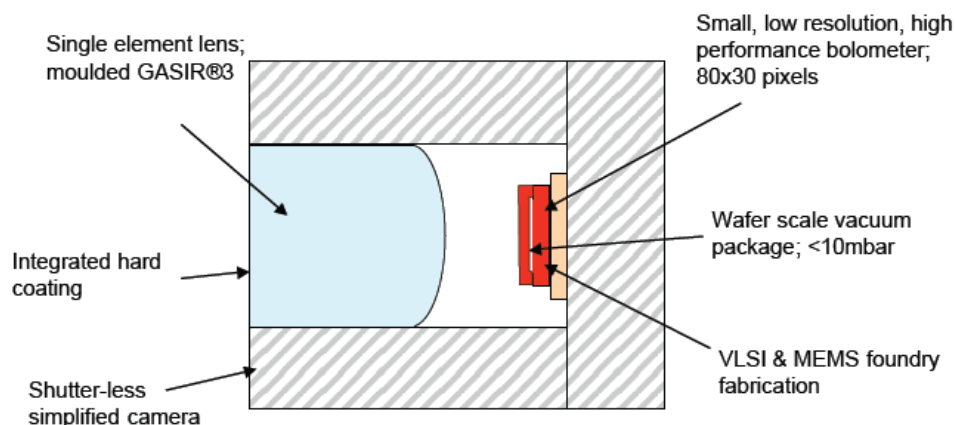
Low-cost uncooled bolometers for market >10 M/Y

Solution:

- Minimize specification requirements
- Develop FIR sensor system based on MEMS mass-fabrication processes



Low-cost FIR camera concept



Single lens design reduce the cost of optics manufacturing

Molding of GASIR® / $n=2.5$

- Chalcogenide glass = low cost input material
- Molded directly into finished optics with high surface quality
- Spherical, aspherical, diffractive
- 2-3 mm focal length
- $f/\# < 1$ possible

Hard coating

- DLC



Product Data Sheet **Fever Scan M3000**

The CANTRONIC Systems Inc. **Fever Scan M3000** system designed for mass screening of public areas for individuals with elevated body temperatures. As a group of people walk past the camera head a thermal image is displayed. Body temperatures above a predefined value, such as a fever, can be visually identified and then further assessed by medical personnel.

The M3000 is a dynamic real time thermal imaging camera system that is capable of evaluating hundreds of people a minute, so pedestrian flow is not restricted. The Fever Scan M3000 is ideal for mass screening for the fever like symptoms, a key indicator of SARS (Severe Acute Respiratory Syndrome), in areas like airports, railway or subway stations, sea ports, and any other public facilities.

Main Features:



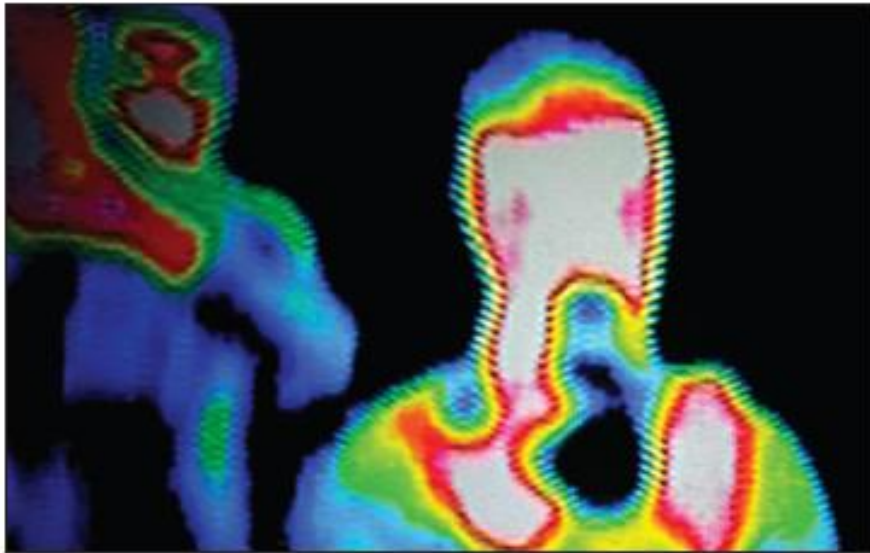
DETAILED FEATURES

- Camera Head:**
- Lens: 50mm
- Focal Plane Array: Micro-bolometer (Amorphous silicon or vanadium oxide)
- Spectral Range: 8-14 μ m
- Number of Pixels: 320X240
- NETD: 0.08°C @ 30°C

- Software User Interface:**
- Data Display: 640x480 on screen/processing
- Visual Alarm: User definable temperature scale and alarm trigger point.
- Alarm Function: Ignore Mode or Save Alarm Mode(saves image to hard drive and log file for easy retrieval/review)
- Options: VGA Monitor, Printer, Tripod

Black Diamond™ Infrared Lenses

LightPath's Black Diamond lenses are infrared lenses manufactured from moldable chalcogenide glass. This glass can be customized for applications between 1 micron to 14 microns in wavelength, opening up new applications in thermal imaging and smart sensors. The lenses can be customized in sizes up to 25mm and can be provided molded into a metal holder or with a diffractive surface to make the systems achromatic.



Black Diamond Manufacturing Tolerances

Parameter	Precision
Center Thickness (CT)	$\pm 0.025\text{mm}$
Diameter	$+ 0 / -0.020\text{mm}$
Decentration	$\pm 0.010\text{mm}$
Wedge	$< 2.5 \text{ arcmin}$
Power/Irregularity	$1 / 0.5 \text{ fringes at } 633\text{nm}$
Roughness	10nm
Refractive Index*	± 0.0005

* Manufacturability depends on size and shape of the optics, as well as production volume.

